Ultrathin CVD Cu Seed Layer Formation Using Copper Oxynitride Deposition and Room Temperature Remote Hydrogen Plasma Reduction

Journal of The Electrochemical Society, **155** (7) H496-H503 (2008)
0013-4651/2008/155(7)/H496/8/$23.00 © The Electrochemical Society

Ultrathin CVD Cu Seed Layer Formation Using Copper Oxynitride Deposition and Room Temperature Remote Hydrogen Plasma Reduction

Hoon Kim, Harish B. Bhandari, Sheng Xu, and Roy G. Gordon*,z

Department of Chemistry and Chemical Biology, Harvard University, Cambridge, Massachusetts 02138, USA

Cu seed layers for future interconnects must have conformal step coverage, smooth surface morphology, and strong adhesion. Conformal deposition had been achieved by chemical vapor deposition (CVD), but CVD Cu films have rough surfaces and poor adhesion. In this paper, conformal, smooth, adherent, continuous, and thin (<9 nm) Cu films were made by CVD. CuON was deposited from a Cu-amidinate precursor, H_2O, and NH_3 at 140–180°C on Ru. Crystallites in the deposited film have either a Cu_2O or Cu_3N structure depending on the ratio of H_2O to NH_3. As-deposited CuON films have a smooth surface morphology [~0.5 nm root-mean-square (rms) roughness] and are highly conformal (>95% step coverage in 40:1 aspect ratio holes). The CuON films were then reduced with remote hydrogen plasma near room temperature to minimize agglomeration of the thin Cu films during reduction. After reduction, CuON films having a Cu_2O crystal structure showed a higher density Cu film (95%) than those having a Cu_3N crystal structure (84%). Both reduced Cu films had a smooth morphology (~1 nm rms roughness). Thus, deposition of a CuON film having a Cu_2O crystal structure and then reduction with remote hydrogen plasma can make Cu layers that can serve as seed layers of future Cu interconnects.
 [DOI: 10.1149/1.2912326]

Manuscript submitted January 18, 2008; revised manuscript received February 15, 2008. Available electronically May 5, 2008.

Cu is used as the interconnect material for ultralarge-scale integrated circuits due to its low resistivity and excellent stability against stress migration and electromigration. Cu is filled by electrochemical deposition (ECD), which has the merits of a low process temperature, a high deposition rate, a cost effective process, and a complete via filling capability. This ECD method requires a thin Cu seed layer as an electrode. In current technology, the Cu seed layer is deposited by sputtering on Ta over a TaN diffusion barrier. However, beyond the 45 nm generation, sputtering cannot cover the sidewalls of vias and trenches uniformly due to its poor step coverage, which results in void formation during ECD and a reduced durability of interconnects.[1] Thus, a conformal deposition method for Cu seed layer deposition is required.[2] Chemical vapor deposition (CVD) and atomic layer deposition (ALD) are well-known methods of conformal Cu seed layer deposition.[3-9] From the viewpoint of productivity, CVD is the most promising candidate for Cu seed layer deposition. For the 32 nm generation, considering the metal linewidth (~32 nm) and the thickness of the barrier/cladding (2.4 nm), a conformal, smooth, adherent, and continuous CVD Cu seed layer less than 10 nm thick is required.[10]

To deposit 10 nm of continuous CVD Cu, new underlayers should be considered because Ta/TaN underlayers cause a rough morphology and poor adhesion.[4,5] Ru is an air-stable metal with a low resistivity and no solubility in Cu, and it does not form any intermetallic compounds with Cu.[11] More importantly, Ru has a strong adhesion to CVD Cu compared with Ta or TaN.[6,7,12,13] Although Cu has a fairly high wettability on Ru, 10 nm of continuous CVD Cu seed layer cannot be deposited on Ru, because metallic Cu made by CVD has typical three-dimensional (3D) island growth and requires a thickness of at least 20 nm to form a continuous layer.[5]

To deposit a thin (<10 nm), smooth, and continuous CVD seed layer, a different approach is required. Cu compounds, such as Cu oxide or nitride, have a better wettability than metallic Cu, which results in a higher nucleation density, and continuous thin layers with a smoother and more continuous morphology than metallic Cu. There is a report of CVD Cu_2O deposition for seed layer application.[14] However, the reduction process temperature is 275°C, which is too high to form a thin, continuous, and smooth seed layer for future Cu interconnect processing. The Ta underlayer used for that experiment is oxidized during oxide deposition, which decreases the adhesion strength of Cu to Ta and increases the contact resistance. Thus, there is need for a new precursor having a low deposition temperature and a new underlayer that can be easily reduced. Deposition of Cu_3N can also be a good candidate. ALD Cu_3N deposition and reduction shows the possibility of thin seed layer fabrication,[15,16] but ALD is too slow for large-scale production. The reported CVD process for Cu_3N required a high deposition temperature (400°C) and it did not mention the morphology, which is most important in this application.[17]

Reduction of a deposited Cu_2O or Cu_3N film to copper metal must be done at a low enough temperature to avoid agglomeration of the Cu. The reduction of a Cu oxide or nitride at too high a temperature produces rough and discontinuous Cu films.[14,15,18,19] Thus, the reduction of Cu compounds should be conducted at as low a temperature as possible to maintain the smooth and continuous morphology of as-deposited Cu compound films.

In this study, we deposited Cu oxide, nitride, and oxynitride (CuON) using CVD, and then these compounds were compared from the viewpoint of morphology and film density before and after reduction to copper metal. A Cu amidinate, (*N*,*N*′-di-*sec*-butylacetamidinato)copper(I) dimer (abbreviated $[Cu(^sBu\text{-}Me\text{-}amd)]_2$), was used to decrease the deposition temperature. This precursor's reactivity at a low substrate temperature has been reported under ALD conditions.[9,15] Cu oxide, Cu nitride, and CuON are formed by using Cu amidinate with H_2O and NH_3 as reactant gases.

The Cu compound films were then reduced by H_2 remote-plasma treatment because atomic hydrogen is one of the strongest reducing agents, which can enable room temperature reduction and minimize agglomeration of the copper.[19,20] Cu_2O reacts with atomic hydrogen to form pure Cu and water by the following reaction

$$Cu_2O + 2H \rightarrow 2Cu + H_2O \quad [1]$$

Provided that no kinetic limitations exist, this reaction will occur because the Gibbs energy change of this reaction is −118.3 kcal/mol at 25°C.[21] Thus, Cu_2O might be reduced with atomic hydrogen even at room temperature.

In this work, we found that the crystal structure of as-deposited CuON films differed depending upon the ratios of H_2O to NH_3 during depositions. A high H_2O ratio makes films with a Cu_2O crystal structure, while a high NH_3 ratio makes a Cu_3N crystal structure. Even though a film has a Cu_2O or Cu_3N crystal structure, both oxygen and nitrogen are incorporated in the film when a mixture of H_2O and NH_3 is used as a reactant gas during deposition. However,

* Electrochemical Society Active Member.
z E-mail: gordon@chemistry.harvard.edu

the overall deposition rate of the film is mainly determined by the H_2O flow rate. CuON film shows a smooth surface morphology [root-mean-square (rms) roughness < 1 nm]. CuON films having Cu_2O structure have higher density than films having Cu_3N structure. After 1 min reduction with H_2 remote plasma at room temperature, both films are fully reduced to Cu metal that has smooth morphology (rms roughness ~ 1 nm) and low resistivity (12 $\mu\Omega$ cm at 9 nm thickness). CVD CuON films having Cu_2O structure form Cu with higher density after reduction than CuON films having Cu_3N structure do. Room temperature remote hydrogen plasma reduction is the best method to maintain smooth surface morphology. Thus, this process can be a promising candidate of thin CVD Cu seed layer deposition for future Cu interconnects.

Experimental

The deposition of CuON was done in a tube-furnace type reactor which has 36 mm inner diameter (i.d.). Copper (I) *N*,*N*′-di-*sec*-butylacetamidinate ($[Cu(^sBu\text{-}Me\text{-}amd)]_2$) was used as a Cu precursor, which was delivered by bubbling with 40 sccm of N_2 carrier gas. The bubbler temperature was 130°C, which maintained the Cu precursor as a liquid phase because its melting point is 77°C. All the gas lines, bubbler, and valves were located in an oven which maintained a good temperature uniformity. H_2O was used as an oxygen source, which was evaporated from a reservoir at room temperature without any carrier gas. The flow rate of water vapor was controlled by a needle valve that was calibrated by comparing with the pressure increase of the chamber by a measured N_2 flow rate. NH_3 was supplied as a nitrogen source whose flow rate was controlled by a mass flow controller. The total flow rate of reactant gases (H_2O and NH_3) was maintained at 40 sccm, and the ratio of H_2O to NH_3 was set to the values 40:0, 30:10, 20:20, 10:30, or 0:40. The reaction gases were mixed with Cu precursor vapor in a small (5 mm i.d.) tube just prior to entering the reactor tube (36 mm i.d.) to ensure thorough mixing. The films were deposited at substrate temperatures from 140 to 220°C under a total chamber pressure of 8 Torr. The films were reduced with H_2 remote plasma, which heated the substrates from room temperature to temperatures as high as 50°C. A toroidal plasma generator (ASTRON I type AX7670, MKS) was supplied with 180 sccm of Ar for plasma ignition and 200 sccm of H_2, which upon dissociative excitation acted as a reducing agent. The reduction time was varied from 30 to 180 s. A Si wafer with a 100 nm thermal oxide was used as the substrate. Ru was deposited by sputtering to a 20 nm thickness and exposed to the atmosphere prior to CVD.

The surface morphologies of the as-deposited CuON and reduced films were evaluated by an atomic force microscope (AFM, Asylum MFP-3D AFM). The thickness and composition of the deposited films were measured using 2 MeV He^+ Rutherford backscattering spectroscopy (RBS). The physical thicknesses of CuON and reduced Cu films were measured by AFM after making stripe patterns by photolithography and etching in dilute nitric acid. CuON and Cu films were etched with nitric acid diluted by deionized water in a volume ratio 1(acid):40(water) or 1:10, respectively. The resistivities of reduced Cu films were evaluated by a four-point probe (Miller Design & Equipment FPP-5000). The phases of as-deposited Cu oxynitride and reduced films were evaluated by transmission electron microscopy (TEM) diffraction (JEOL JEL2010 TEM) using as a substrate a 50 nm thick Si_3N_4 membrane TEM grid (Ted Pella, Inc., prod. no. 21500–10).

Results and Discussion

Cu oxynitride deposition with $[Cu(^sBu\text{-}Me\text{-}amd)]_2$, H_2O, and NH_3.— Temperature effect on CuON film deposition.— CuON was deposited from $[Cu(^sBu\text{-}Me\text{-}amd)]_2$ vapor and a mixture of H_2O vapor and NH_3 gas. Figure 1 shows the deposition rate of Cu oxynitride at different deposition temperatures. The ratio of H_2O flow to NH_3 flow was 30:10 in these depositions. The deposition rate increased with increasing deposition temperature, up to a value over 4 nm min^{-1}. Over the range of temperature studied (140–220°C), the deposition rate has an Arrhenius form, which means that the CVD reaction is kinetically controlled in that temperature range. The activation energy of this reaction was found to be 44 kJ/mol.

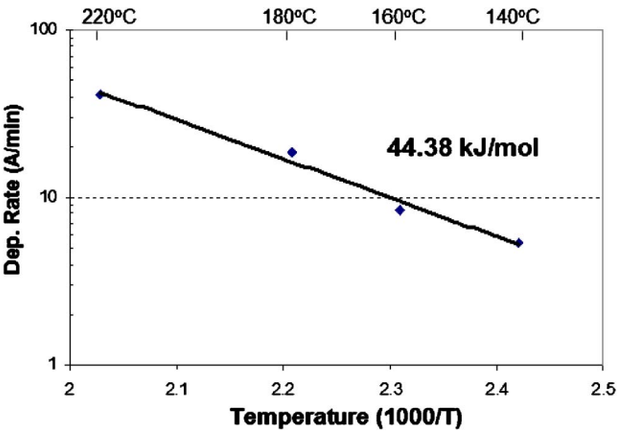

Figure 1. (Color online) Arrhenius plot of CuON deposition rate from $[Cu(^sBu\text{-}Me\text{-}amd)]_2$ vapor and a mixture of 30 sccm of H_2O and 10 sccm of NH_3.

The morphology of CuON depends on the deposition temperature, as shown in Fig. 2 for films with thicknesses about 20 nm. These films are all smooth, with a rms roughness <1 nm. The smoothest film was deposited at 160°C, with a roughness of only 0.5 nm, which is just slightly larger than the roughness of the Si substrate. The surface grain size of CuON is constant at about 20 nm up to a deposition temperature of 180°C. At 220°C, some large particles 400–600 nm in diameter were observed on the film surface, although the film still had a smooth surface morphology (rms roughness 1.04 nm) and a fairly small grain size ($\sim$40 nm). These particles seemed to be formed by gas-phase reaction at the highest temperature. Thus, CuON for a seed layer can be deposited over the temperature range from about 140–180°C from the viewpoint of surface morphology. This result is different from the temperature effect on morphology of Cu_2O and Cu_3N. The morphology of pure Cu compounds such as Cu_2O and Cu_3N was very sensitive to deposition temperature.[15,19] A deposition temperature only 30 or 40°C higher than the optimized condition always made films with a rough morphology in the deposition of pure Cu compounds. However, CuON is less affected by deposition temperature, so smooth CuON films are obtained over a wider process window than for Cu_2O or Cu_3N films.

The composition of CuON deposited at different temperatures is shown in Fig. 3. The atomic percentages of Cu, O, and N are compared at 140, 180, and 220°C as measured by RBS for films deposited on amorphous carbon substrates. The composition does not change much over that temperature range, which means that CuON is a stable phase under these deposition conditions. Thus, CuON has a relatively wide process window in which to get a uniform composition and morphology because it is less sensitive to the deposition temperature. Pure Cu_2O and Cu_3N showed a single phase and smooth morphology only in a narrower temperature range.[15,19]

The effect of H_2O to NH_3 ratio on CuON film deposition.— The deposition rate of CuON depends on the H_2O to NH_3 ratio at 140°C as shown in Fig. 4. The deposition rate is mainly determined by the H_2O flow rate, showing that H_2O is more reactive than NH_3 with the Cu amidinate precursor. Without H_2O, no film was deposited at 140°C, which shows that the Cu precursor and NH_3 alone cannot nucleate a Cu_3N film at 140°C. At substrate temperatures over 200°C, some Cu_3N film was deposited, but it has a very rough morphology. Thus, CuON film was investigated due to its smoother morphology and higher deposition rate.

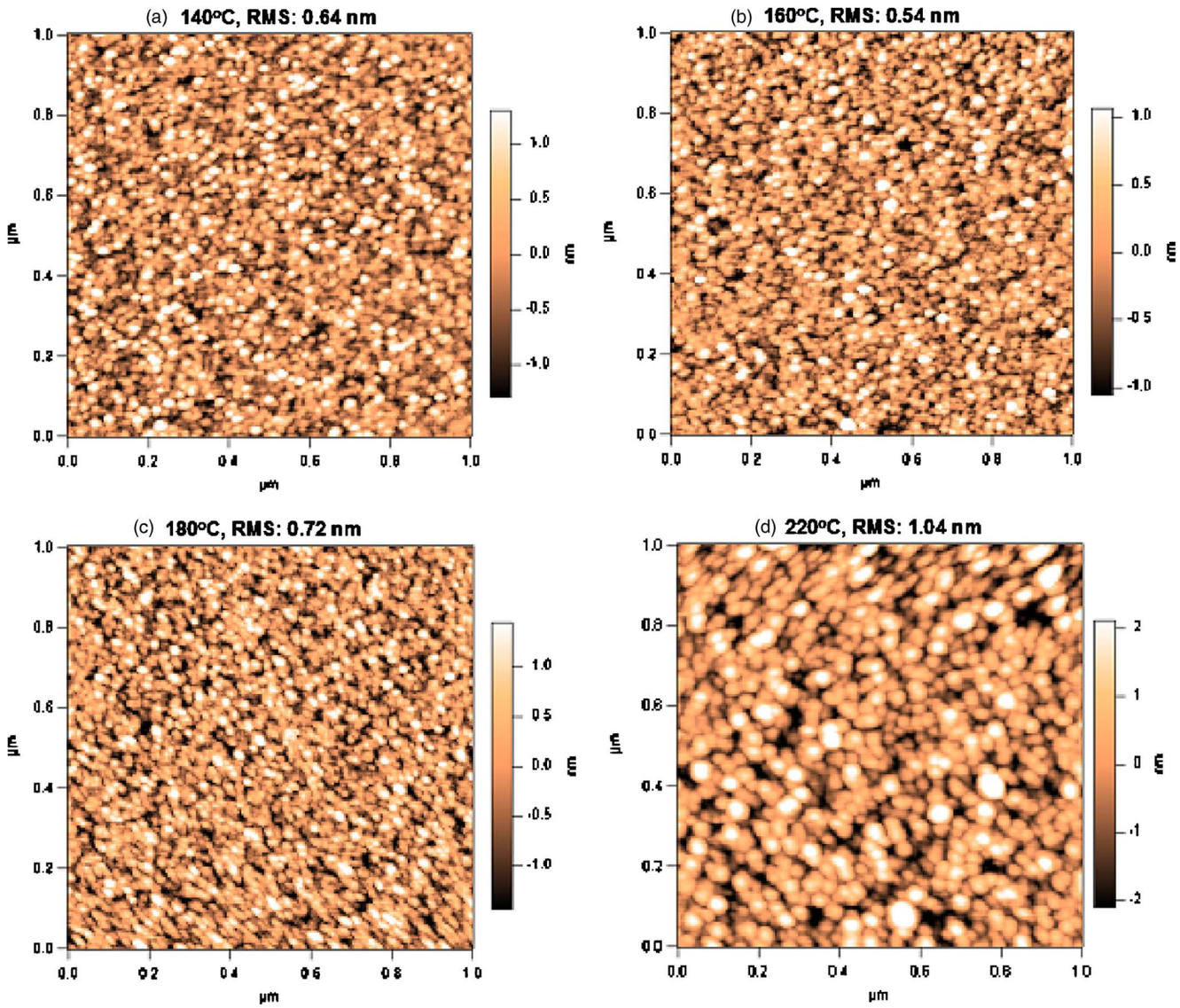

Figure 2. (Color online) AFM images of CuON films grown from $[Cu(^sBu\text{-}Me\text{-}amd)]_2$ vapor and a mixture of 30 sccm of H_2O and 10 sccm of NH_3 at (a) 140, (b) 160, (c) 180, and (d) 220°C, which have about 20 nm thickness.

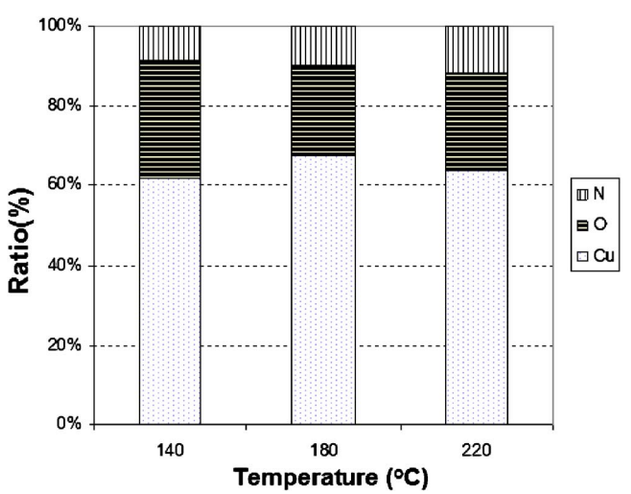

Figure 3. (Color online) The composition of CuON films deposited on carbon substrates from $[Cu(^sBu\text{-}Me\text{-}amd)]_2$ vapor and a mixture of 30 sccm of H_2O and 10 sccm of NH_3 at different temperatures, as measured by RBS.

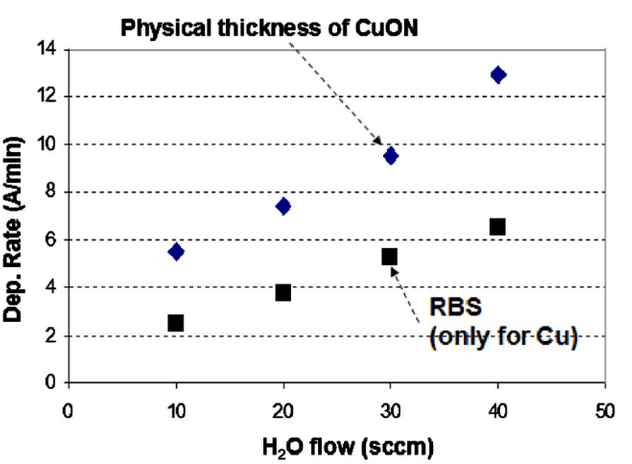

Figure 4. (Color online) Deposition rate of CuON film at different H_2O and NH_3 ratios at 140°C, 8 Torr working pressure. Total flow rate of H_2O and NH_3 is maintained at 40 sccm. Thus, the NH_3 flow rate is equal to 40 sccm minus the H_2O flow rate.

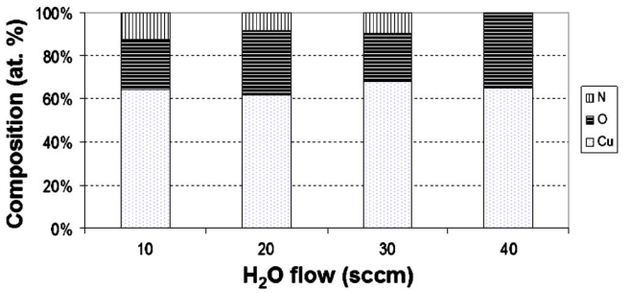

Figure 5. (Color online) Composition of CuON films deposited with different H_2O to NH_3 ratios at 140°C, 8 Torr working pressure. The NH_3 flow rate is equal to 40 sccm minus the H_2O flow rate. The composition was measured by RBS from films deposited on amorphous carbon substrates.

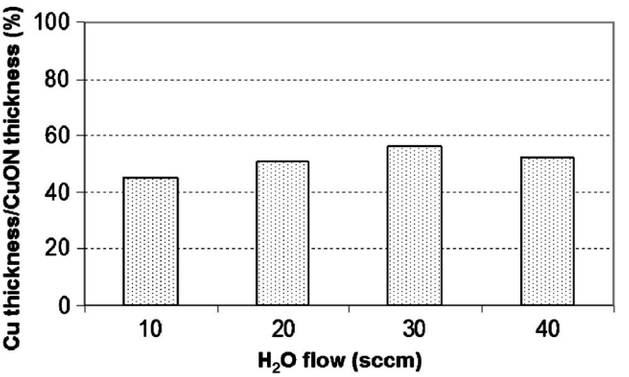

Figure 6. The ratio of Cu in the CuON film for different H_2O and NH_3 flow rates. The Cu ratio is defined by the ratio of Cu thickness (from RBS and calculated at the bulk density of Cu) to physical thickness of CuON.

Compositions of CuON films deposited with different H_2O to NH_3 ratios at 140°C are shown in Fig. 5. The oxygen content of the films exceeds the nitrogen content, even for the film grown from an excess of ammonia (H_2O to NH_3 flow ratio of 10:30). This is another indicator that water vapor is more reactive with the copper precursor than ammonia is. If we assign the conventional oxidation states to O (−2) and N (−3), these compositions all correspond closely to copper in the +1 oxidation state. Because the copper in the precursor is also in the +1 oxidation state, the reactions with H_2O and NH_3 do not produce any oxidation or reduction of the copper during CVD of the films.

The "Cu ratio" is defined by the ratio of Cu thickness to physical thickness of CuON. The physical thickness of CuON film was measured by AFM after etching a stripe pattern. Cu thickness was measured by RBS and calculated as if it were pure copper with bulk density. From Fig. 6 the Cu ratio in the CuON films reached a maximum for the conditions of 30 sccm of H_2O and 10 sccm of NH_3. Films with a high Cu ratio contain more Cu that may be obtained by the reduction of a given thickness of CuON.

All the CuON films have a very smooth surface morphology. The morphology of deposited CuON depends on the ratio of H_2O to NH_3 as shown in Fig. 7. With increasing the H_2O ratio, the grain size increased, but the rms roughness value decreased, so the grains became wider, flatter, and less tall.

The crystal structure of CuON film depended on the ratio of flow rates of H_2O to NH_3. The structure was evaluated by electron diffraction in a TEM image (Fig. 8). The diffraction patterns were obtained from CuON films deposited in three different conditions: Fig. 8a for 10 sccm H_2O and 30 sccm NH_3, Fig. 8b for 30 sccm H_2O and 10 sccm NH_3, and Fig. 8c for 40 sccm H_2O. The electron diffraction pattern of Fig. 8a (high NH_3) matches with the Cu_3N structure.[22] Those of Fig. 8b and c (high H_2O) coincide with the crystal structure of Cu_2O.[23] The peak assignments are summarized in Tables I and II for the Cu_3N and Cu_2O structures, respectively. Although the CuON films have similar compositions, the films show different crystal structures. The high ratio of NH_3 only makes a Cu_3N structure, even though that film contains 24 atom % oxygen. The high ratio of H_2O makes CuON films having only the crystal structure of Cu_2O. We find no additional diffraction peaks that could arise from a crystalline mixed oxynitride phase, nor did we find any such phases reported. Thus, it seems likely that these films contain a significant amount of amorphous copper oxynitride that only has broad diffraction patterns and a smooth surface morphology.

It is thought that H_2O reacts with the Cu precursor on a surface, followed by the reaction of NH_3 with Cu–O on the surface because CuON film is not deposited without H_2O. Thus, a high NH_3 flow and low H_2O flow make a low deposition rate of Cu_2O, causing a longer time for NH_3 reaction on the surface, which results in the formation of a Cu_3N structure containing oxygen. This result coincides with ALD Cu_3N deposition using a pulse sequence of Cu precusor/H_2O/NH_3.[16] Torndahl et al.[16] made Cu oxide, first using $Cu(hfac)_2$ and H_2O; then it was nitrified by a NH_3 pulse, which resulted in the formation of Cu_3N. Thus, Cu_2O and Cu_3N can be formed by controlling the reaction gas ratio because the kinetic competition between H_2O and NH_3 with Cu atoms on the surface can make both structures.

The step coverage of CVD CuON was tested by depositing film on a silicon substrate with holes having aspect ratios of 40:1. The scanning electron microscopy (SEM) image of a cleaved cross section in Fig. 9 shows a step coverage of about 95% at the bottom of these very narrow holes.

Reduction of CuON with remote H_2 plasma at room temperature.— CuON films can be deposited with different crystal structures and Cu densities depending on the ratio of H_2O to NH_3. The CuON film (high H_2O CuON) with high H_2O ratio (H_2O:30 sccm, NH_3:10 sccm) has a Cu_2O crystal structure and a high Cu ratio (53%). Low H_2O CuON from low H_2O ratio (H_2O:10 sccm, NH_3:30 sccm) has the crystal structure of Cu_3N and a low Cu ratio (41%). Thus, these two films were used to compare the reduction behavior because these can represent high or low density films. High H_2O CuON has about a 12% higher Cu ratio than that of low H_2O CuON.

The CuON films were reduced with remote H_2 plasma. The films were not heated deliberately, but their temperature did rise from room temperature to about 50°C because of the heat released by the recombination of hydrogen atoms to form H_2 and by reaction with oxygen and nitrogen on CuON surfaces. The as-deposited thicknesses of these high H_2O CuON and low H_2O CuON films were 16 and 14 nm, respectively. The sheet resistance of the films depends on reduction time as shown in Fig. 10. After 1 min reduction treatment, both CuON films were reduced to Cu. The sheet resistance is not changed further after 3 min reduction, which means that reduction for 1 min is sufficient to reduce 14–16 nm thick CuON films with either crystal structure. The morphology of reduced CuON was evaluated by AFM, shown in Fig. 11. Both high H_2O and low H_2O CuON a showed smooth surface morphology (1.1–1.2 nm rms roughness) even after 3 min reduction. Thus, the reduced Cu films were not agglomerated even at a longer reduction time. Because the films retain their smooth morphology even after over-reduction for longer times, we expect that films can also be reduced successfully inside the whole length of deep trenches. Film near the top of a trench will be reduced before film deeper in the trench, which only receives a smaller flux of hydrogen atoms depleted by reactions at the walls during their diffusion down the trench.

Because these films were reduced at nearly room temperature, they can maintain their smooth surface morphology by avoiding diffusion of the Cu over the Ru surface to form agglomerates. How-

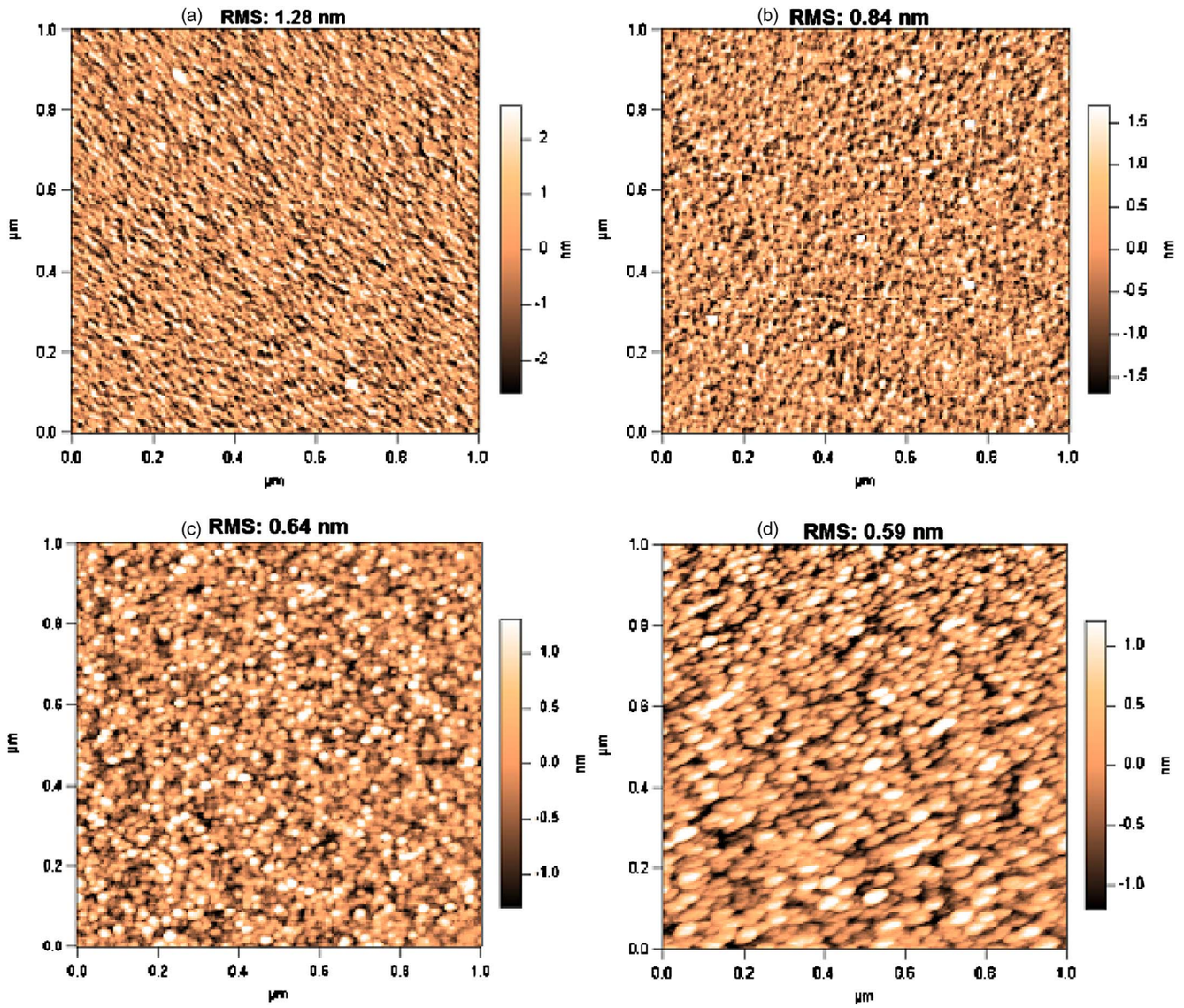

Figure 7. (Color online) AFM image of CuON film grown at 140°C with the flow rate of H_2O and NH_3; (a) 10:30, (b) 20:20, (c) 30:10, and (d) 40:0 sccm.

ever, CuON films deposited on SiO_2 underlayers were agglomerated under the same reduction condition, as shown by the increase in rms roughness from 0.7 to ~3.5 nm (Fig. 12). Any surface oxide on ruthenium can be reduced during the CuON reduction because the stabilities of Cu_2O and RuO_2 are similar. The Gibbs energies of the reduction reactions for these oxides are similar,[21] which implies both metal oxides can be reduced under similar reduction conditions. The Cu is bonded strongly to the reduced metallic surface of Ru. However, Cu on Si having a native oxide can be agglomerated during reduction even at room temperature due to the high mobility of Cu atoms on oxide surfaces[9] and the difficulty of reducing silicon oxides. Thus, an easily reducible underlayer like Ru is essential for maintaining a smooth surface morphology during the reduction of CuON.

The volume shrinkage of two CuON films was evaluated by comparing the thickness of CuON film before and after reduction. The physical thickness of high H_2O CuON is changed from 16 to 9 nm, which is a shrinkage of volume by 45%. Low H_2O CuON showed that the thickness is changed from 14 to 7 nm, which means a 50% volume shrinkage. These samples are evaluated by RBS to measure the density of reduced Cu film. The RBS result shows that the thickness of high or low H_2O CuON would be 8.5 or 5.9 nm, respectively, if they had bulk Cu density. Thus, comparing these values with the physical thicknesses, the density of the reduced copper from high Cu_2O CuON or low H_2O CuON is 95 or 84%, respectively, of the bulk value. Summarizing the density of the CuON films, high Cu_2O CuON has a higher density not only in the as-deposited film but also after reduction. Thus, high Cu_2O CuON film should be used as the most suitable Cu compound for reduction to deposit a dense, reduced Cu film.

The resistivity of reduced high Cu_2O CuON is 12 $\mu\Omega$ cm at a thickness of 9 nm. That of low H_2O CuON film has 15 $\mu\Omega$ cm at a thickness of 7 nm. These values are similar to the resistivity of sputtered Cu at the corresponding thicknesses.[15] Thus, the reduced Cu film has a high density and high purity.

All the reduced copper films on ruthenium pass the tape test for adhesion, whereas the ones on silica are easily pulled off by tape. More quantitative 4-point bend tests of adhesion are underway.

Conclusions

Smooth, continuous, dense, and conformal Cu films with ~1 nm rms roughness and thickness <10 nm were fabricated by

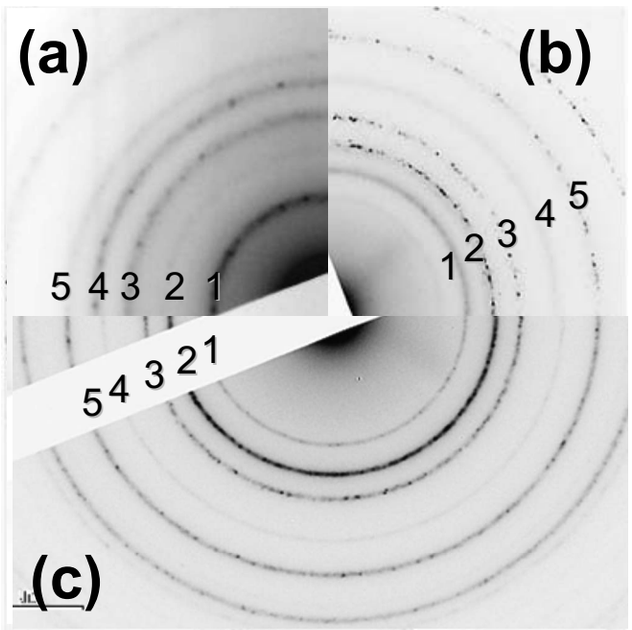

Figure 8. TEM diffraction pattern of CuON films grown at 140°C with the flow rate of H_2O and NH_3 at (a) 10:30, (b) 30:10, and (c) 40:0 sccm.

CVD of CuON followed by reduction with remote hydrogen plasma at room temperature. The crystal structure of CuON can be controlled by the ratio of H_2O and NH_3, although the elemental composition of the film was not changed significantly. A high H_2O ratio makes the CuON film having a Cu_2O crystal structure. A low H_2O ratio, meaning high NH_3 partial pressure, makes CuON films having a Cu_3N crystal structure. The reduction rate of the films does not show any difference depending on the crystal structure. CuON film with a Cu_2O structure produces a higher density of Cu after reduction. Thus, CuON having a Cu_2O structure is the best Cu compound

Table I. Electron diffraction results for low H_2O CuON film from TEM. The index of plane (*hkl*) and interplanar spacing (*d*) shown in this table represents the Cu_3N crystal structure. Error means the difference between reference data and measured data.

No.	*hkl*	*d* (A)	Int.	Measured *d* (A)	Error (%)
1	100	3.82	60	3.83	−0.26
2	110	2.70	30	2.69	0.21
3	111	2.20	100	2.20	−0.02
4	200	1.91	80	1.91	−0.29
5	210	1.71	30	1.69	0.89

Table II. Electron diffraction result for high H_2O CuON film from TEM. The index of plane (*hkl*) and interplanar spacing (*d*) shown in this table represents the Cu_2O crystal structure. Error means the difference between reference data and measured data.

No.	*hkl*	*d* (A)	Int.	Measured *d* (A)	Error (%)
1	110	3.04	20	3.03	0.32
2	111	2.46	100	2.46	0.04
3	200	2.14	70	2.14	−0.13
4	211	1.74	20	1.74	−0.24
5	220	1.51	90	1.50	0.66

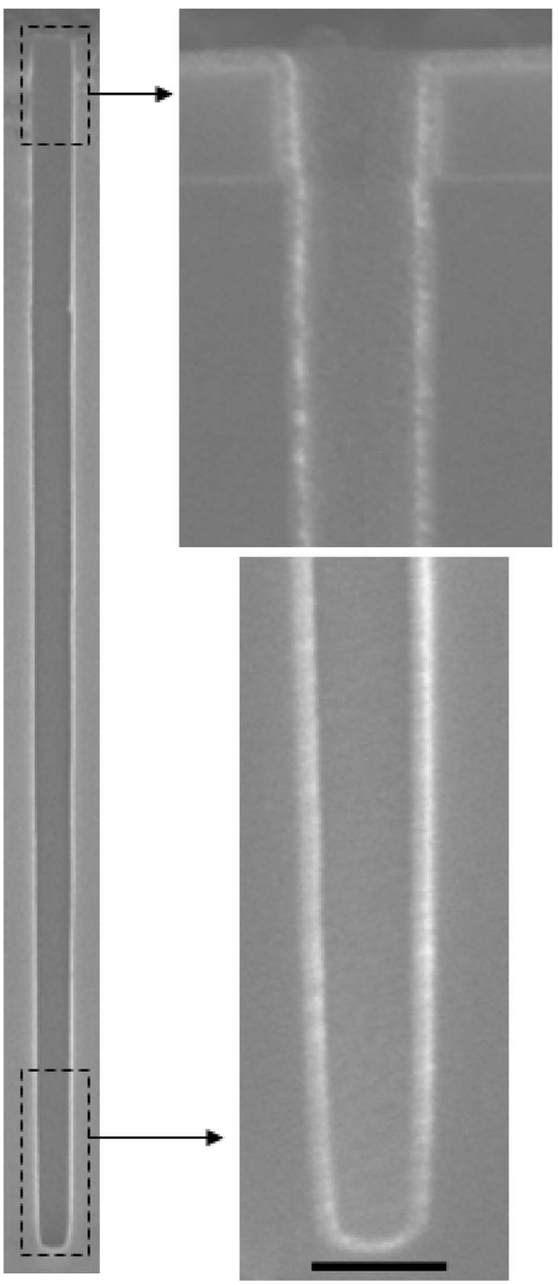

Figure 9. SEM image of a CuON film deposited at 140°C with 30 sccm of H_2O and 10 sccm of NH_3 on an oval hole (diameter 0.13 × 0.19 μm, length 6.7 μm). Scale bar is 200 nm.

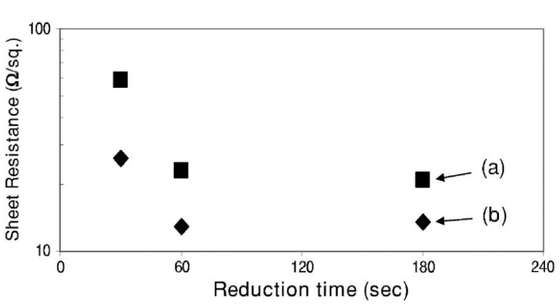

Figure 10. Sheet resistance of (a) low and (b) high H_2O CuON film depending on reduction time at room temperature.

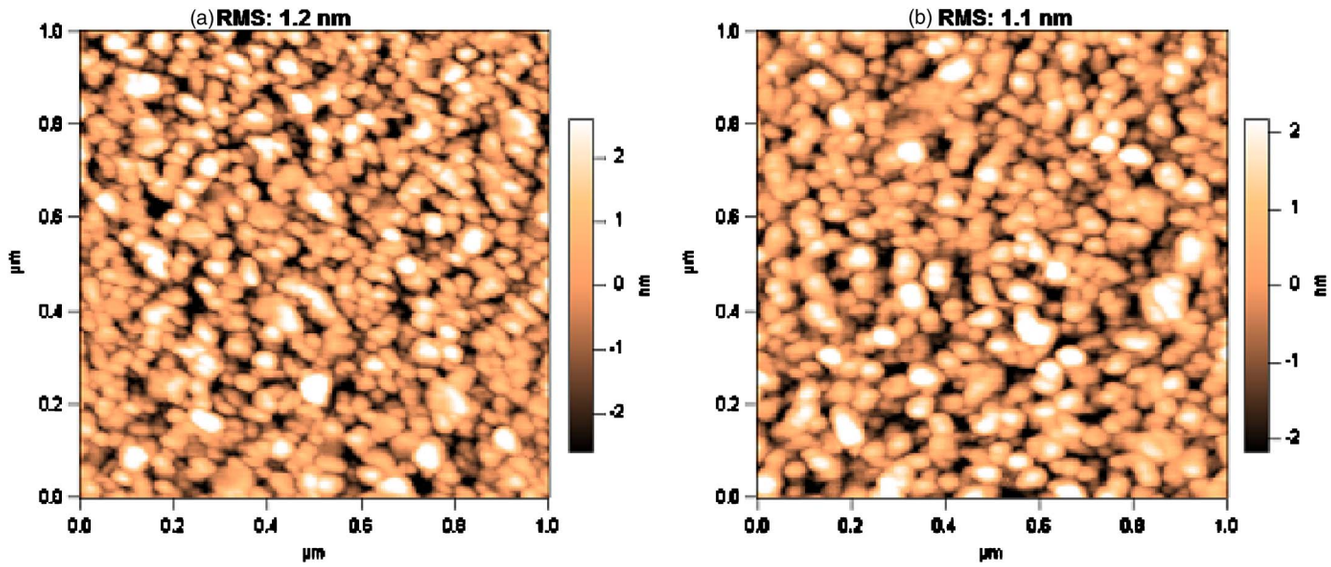

Figure 11. (Color online) AFM image of reduced Cu films from (a) low and (b) high H_2O CuON at room temperature for 3 min on Ru substrates.

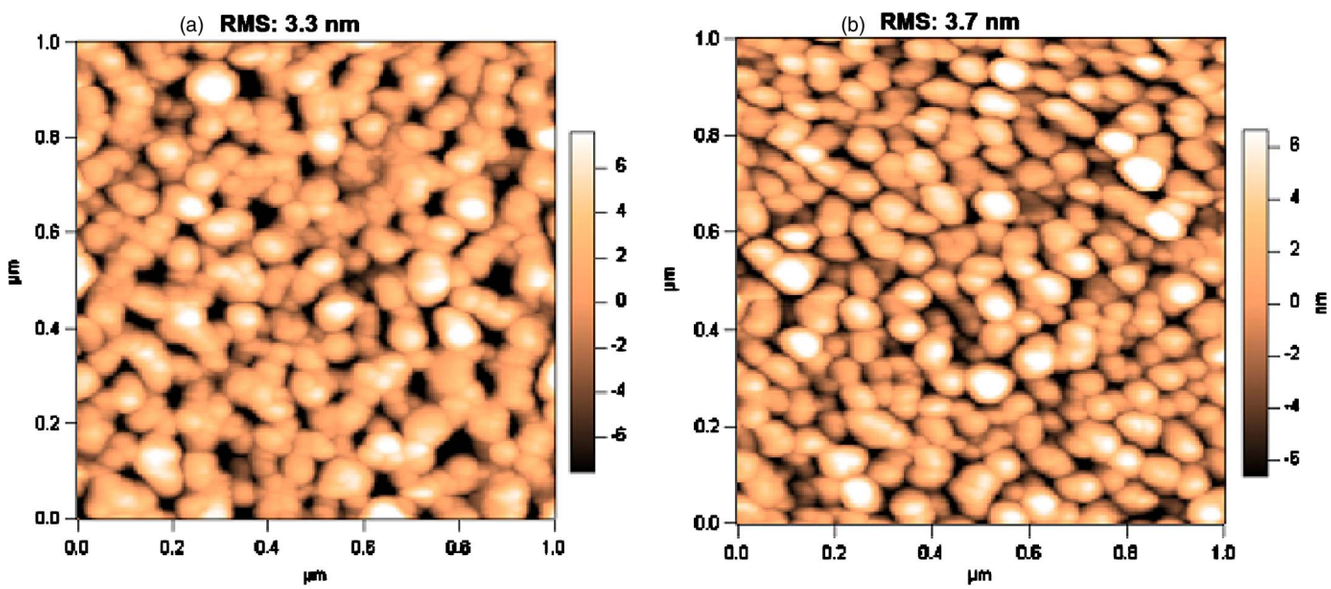

Figure 12. (Color online) AFM image of reduced Cu films from (a) low and (b) high H_2O CuON at room temperature for 3 min on SiO_2 substrates.

for this deposition and reduction process, which is a promising method for Cu seed layer deposition for future Cu interconnects.

Acknowledgments

The copper precursor was supplied by the Advanced Thin-Film Technologies Group, Rohm and Haas Electronic Materials. Silicon substrates with deep trenches were supplied by Qimonda. Support for this work was provided by the Rohm and Haas Company, Intel Corporation, and the National Science Foundation.

Harvard University assisted in meeting the publication costs of this article.

References

1. R. Rosenberg, D. C. Edelstein, C.-K. Hu, and K. P. Rodbell, *Annu. Rev. Mater. Sci.*, **30**, 229 (2000).
2. A. H. Simon, S. B. Law, J. B. Tan, S. G. Malhotra, K. S. Lam, S.-C. Seo, and P. Dehaven, in Proceedings of Adv. Met. Conference, Materials Research Society, p. 545 (2004).
3. R. Kroger, M. Eizenberg, D. Cong, N. Yoshida, L. Y. Chen, S. Ramaswami, and D. Carl, *J. Electrochem. Soc.*, **146**, 3248 (1999).
4. Y. S. Kim and Y. Shimogaki, *J. Vac. Sci. Technol. A*, **19**, 2642 (2001).
5. H. Kim and Y. Shimogaki, *J. Electrochem. Soc.*, **154**, G13 (2007).
6. O. K. Kwon, J. H. Kim, H. S. Park, and S. W. Kang, *J. Electrochem. Soc.*, **151**, G109 (2004).
7. H. Kim, Y. Kojima, H. Sato, N. Yoshii, S. Hosaka, and Y. Shimogaki, *Jpn. J. Appl. Phys., Part 2*, **45**, L233 (2006).
8. R. Solanki and B. Pathangey, *Electrochem. Solid-State Lett.*, **3**, 479 (2000).
9. Z. Li, A. Rahtu, and R. G. Gordon, *J. Electrochem. Soc.*, **153**, C787 (2006).
10. Semiconductor Industry Association, International Technology Roadmap for Semiconductors, 2007 ed., SEMATECH, Austin, TX (2007).
11. P. R. Subramanian, D. J. Chakrabarti, and D. E. Laughlin, *Phase Diagrams of Binary Copper Alloys*, p. 412, ASM International, Materials Park, OH (1994).
12. H. Kim, T. Koseki, T. Ohba, T. Ohta, Y. Kojima, H. Sato, and Y. Shimogaki, *J. Electrochem. Soc.*, **152**, G594 (2005).
13. H. Kim, Y. Naito T. Koseki, T. Ohba, T. Ohta, Y. Kojima, H. Sato, and Y. Shimogaki, *Jpn. J. Appl. Phys.*, **45**, 2497 (2006).
14. C. Lee and H.-H. Lee, *Electrochem. Solid-State Lett.*, **8**, G5 (2005).
15. Z. Li and R. G. Gordon, *Chem. Vap. Deposition*, **12**, 435 (2006).

16. T. Torndahl, M. Ottosson, and J. Carlsson, *J. Electrochem. Soc.*, **153**, C146 (2006).
17. J. Pinkas, J. C. Huffman, D. V. Baxter, M. H. Chisholm, and K. G. Caulton, *Chem. Mater.*, **7**, 1589 (1995).
18. P. J. Soininen, K.-E. Elers, V. Saanila, S. Kaipio, T. Sajavaara, and S. Haukka, *J. Electrochem. Soc.*, **152**, G122 (2005).
19. H. Kim, Y. Kojima, H. Sato, N. Yoshii, S. Hosaka, and Y. Shimogaki, in Proceedings of Materials Research Society Spring Meeting 2006, Materials Research Society, p. 0914–F05–115 (2006).
20. Y. Sawada, H. Tamaru, M. Kogoma, M. Kawase, and K. Hashimoto, *J. Phys. D*, **29**, 2539 (1996).
21. D. R. Lide, *CRC Handbook of Chemistry and Physics*, 76th ed., p. 1995, CRC Press, Boca Raton, FL (1995–1996).
22. U. Zachwieja and H. Jaconbs, *J. Less-Common Met.*, **161**, 175 (1990).
23. R. Restori and D. Schwarzenbach, *Acta Crystallogr., Sect. B: Struct. Sci.*, **B42**, 201 (1986).